Understanding the interplay between surface properties and the aspect ratio of ellipsoidal nanomaterials

Ahmed Zeeshan, Hicheme Hadji, Hiba Khelifa, Mickael Bourge, Kawthar Bouchemal

Understanding the Interplay Between Surface Properties and the Aspect Ratio of Ellipsoidal Nanomaterials

Ahmed Zeeshan [1#], Hicheme Hadji [1#], Hiba Khelifa,[2] Mickaël Bourge [3], Kawthar Bouchemal [2]*

1. Université Paris-Saclay, IGPS, CNRS UMR 8612, 17 Av. des Sciences, 91190 Orsay, France
2. Chimie ParisTech, PSL University, CNRS, Institut de Recherche de Chimie Paris, 75005 Paris, France
3. Institute for Integrative Biology of the Cell (I2BC), CEA, CNRS, Université Paris-Saclay, Gif-sur-Yvette Cedex, France

*Corresponding author

kawthar.bouchemal@chimieparistech.psl.eu

[#] Equally contributing authors

12

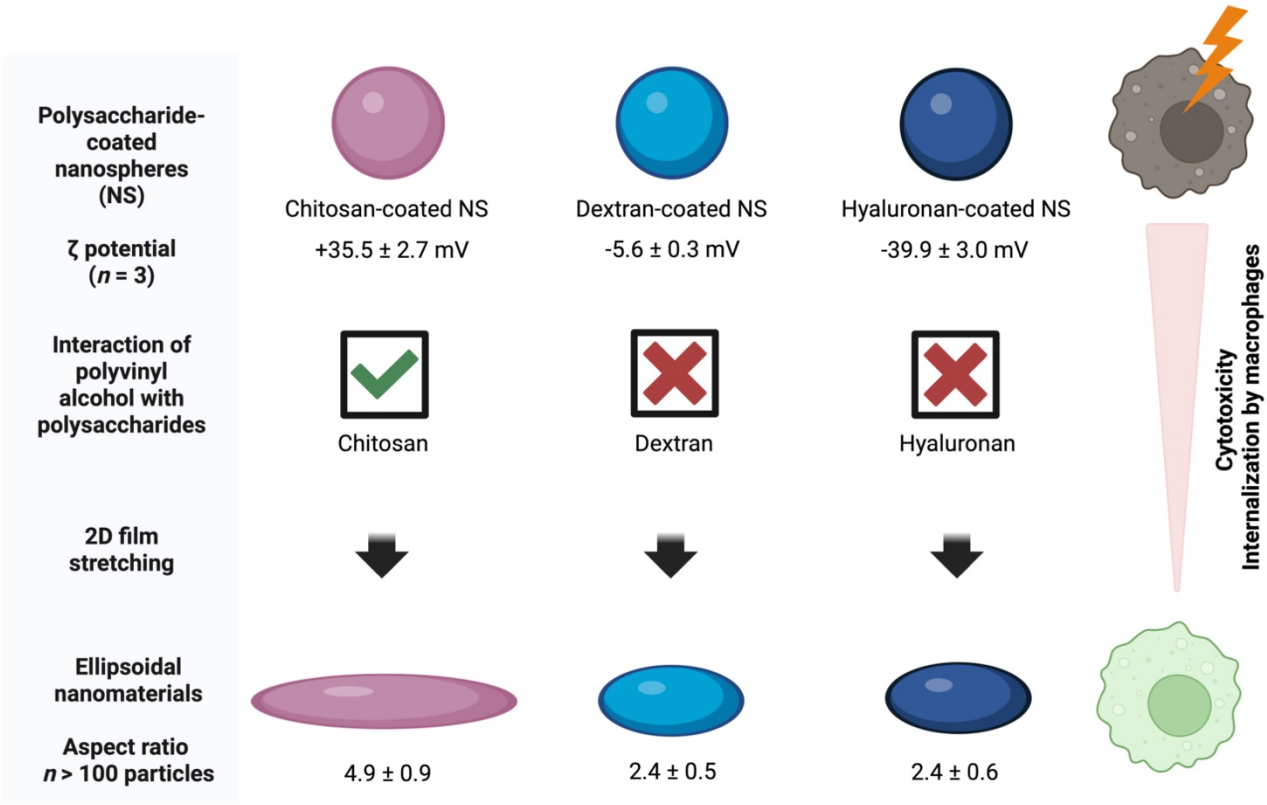

13

14 ***Graphical abstract***

ABSTRACT

Polymeric nanomaterials (NM) with nonspherical morphologies have increasingly captured the spotlight in biomedical applications. Physical deformation of nanospheres (NS) represents a versatile technique for obtaining ellipsoidal NM (E-NM) that exhibit unique properties regarding their interactions with biological systems. Despite this technique's versatility and simplicity, the film's detailed composition and the parameters controlling the efficiency of the NS's physical deformation still need to be clarified. Herein, we detailed a step-by-step formulation of a film composed of polyvinyl alcohol (PVA), and we investigated the impact of NS surface properties on the efficiency of the physical stretching. To reach those objectives, we designed two morphologies (NS and E-NM), and for each morphology, the surface composition was modified by using three different polysaccharides (chitosan, dextran, and hyaluronan). Physicochemical analysis revealed a connection between NS surface potential, their interaction with PVA, and the aspect ratio of ellipsoidal NM. Chitosan-coated E-NM had the highest aspect ratio ($\Gamma = 4.9$), which decreased to 2.4 with dextran and hyaluronan coatings. Isothermal titration calorimetry demonstrated strong interaction between PVA and chitosan but little interaction with dextran and hyaluronan. Finally, the impact of NM morphology and surface properties on phagocytosis showed that E-NM exhibited a reduced internalization by macrophages and reduced cytotoxicity compared to NS. Overall, in this study, we highlighted that the aspect ratio of E-NM is controlled by the strength of the interaction with PVA with the polysaccharide on the NS surface and revealed the role of NM morphology in reducing cytotoxicity and escaping internalization by macrophages.

KEYWORDS: Nanomaterials; Morphology; Surface properties; Cytotoxicity.

Abbreviations

DDA, Degree of deacetylation

DMEM, Bulbecco-modified eagle médium

DMSO, Dimethyl sulfoxide

E-NM, Ellipsoidal nanomaterial

EDC, 1-ethyl-3-(3-dimethylaminopropyl) carbodiimide

FBS, Fetal bovine serum

FITC, Fluorescein isothiocyanate Isomer I

HPLC, High-performance liquid chromatography

IC_{50}, The concentration of polysaccharide preparations to reduce cell viability by 50% relative to untreated control cells

ITC, Isothermal titration calorimetry

J774A.1, Murine monocyte macrophages

MFI, Mean fluorescence intensity

NHS, *N*-hydroxysuccinimide

NM, Nanomaterials

NS, Nanospheres

NS_{PVA}, Nanospheres incubated with PVA and purified by dialysis

PBS, Phosphate buffer saline

PVA, Poly(vinyl alcohol)

QELS, Quasi-Elastic Light Scattering

TEM, Transmission Electron Microscopy

1. INTRODUCTION

Since the 1970s, polymeric nanomaterials (NM) have emerged as promising systems with numerous advantages over conventional formulations.[1, 2] They have shown ground-breaking achievements in improving drug efficacy/toxicity ratio, controlled drug release, and targeted drug biodistribution by efficiently bypassing biological barriers.[3] Among criteria defining synthetic identity, NM morphology has been considered during the last decade as a novel parameter that plays a pivotal role in controlling biological processes.[4, 5] Nevertheless, a close inspection of the literature reveals that most experimental works conducted on nonspherical NM have been devoted to metal[6, 7] or carbon nanotubes,[8] while NM composed of polysaccharides and polymers were less investigated. Among the various techniques used to produce nonspherical NM, the film stretching technique offers the advantage of simultaneously modifying the morphology and surface properties of NM composed of polymers and polysaccharides.[9-12] This technique involves dispersing nanospheres (NS) in a polyvinyl alcohol (PVA) solution, followed by drying and stretching of the resulting PVA film containing the NS. Ellipsoidal particles are then obtained by dissolving the film in water at ambient temperature. PVA is considered a class of water-soluble synthetic polymers, but water solubility primarily depends upon the degree of hydrolysis of the acetate groups in the polyvinyl acetate.

Previous works utilized PVA with a minimum degree of hydrolysis of 87% and a molecular weight of approximately $\approx 115 \times 10^3$ g mol^{-1}.[9] In that study, the films were immersed in an oil bath maintained at 200 °C before stretching. In another publication, the stretching of PVA was performed at a lower temperature (50 °C), using a commercial film known as STBT®.[11, 12] However, the STBT® film contains insoluble debris.[12] The PVA concentration in the STBT® film, the degree of hydrolysis, and the molecular weight are unknown. In this context, herein we report the first step-by-step formulation of the PVA film in which the NS are dispersed before stretching. The PVA molecular

weight, its degree of hydrolysis, the concentration in water, and the concentration of glycerol used as a plasticizer were varied in a rational way.

On the other hand, the parameters leading to efficient film stretching and, consequently, high aspect ratio, still need to be clarified. Several works hypothesized that parent NS's glass transition temperature (T_g) was a crucial parameter for the stretching efficiency.[9, 13] Within this framework, the second objective of this investigation is to understand the effect of NM surface properties and the T_g on the efficiency of the physical deformation of the NS characterized by the aspect ratio of ellipsoidal NM.

To reach those objectives, our strategy is to consider two NM morphologies: spherical particles (nanospheres, NS) and ellipsoidal NM (E-NM). After optimizing the PVA formulation, we investigated three types of polysaccharides for each morphology: chitosan, dextran, and hyaluronan. We selected three preparation types with comparable T_g but varying surface compositions. Spherical particles composed of poly(isobutyl cyanoacrylate) (PIBCA) were obtained by polymerizing isobutyl cyanoacrylate monomer and polysaccharides.[14-17] Shape-persistent E-NM with a high aspect ratio ($\Gamma = 3.4$) were achieved through the physical deformation of NS.[12] The E-NM shape was stable for 6 months at different temperatures (4 °C, 20 °C, and 40 °C).[12] Subsequently, we will characterize the NM's morphology, dimensions, and surface potential. Finally, we will explore the effects of NM morphology and surface composition on cell cytotoxicity and endocytosis.

2. MATERIALS

2.1. Reagents for polysaccharide chemical modification and NM design

Chitosan ($\approx 20 \times 10^3$ g mol^{-1} and degree of deacetylation DDA > 85% according to the manufacturer) was purchased from Amicogen (Seoul, Korea). Hyaluronan ($\approx 61 \times 10^3$ g mol^{-1}) was purchased from Lifecore Biomedical (Minnesota, USA). Dextran ($\approx 64 \times 10^3$ g mol^{-1}), glycerol, polyvinyl alcohol (PVA, fully hydrolyzed, 99% hydrolyzed ($\approx 89 \times 10^3$ - 98×10^3 g mol^{-1}), 80%

hydrolyzed (≈ 9×10^3 - 10×10^3 g mol^{-1}), and 87 - 90% hydrolyzed (≈ 30×10^3 - 70×10^3 g mol^{-1})), 1-ethyl-3-(3-dimethylaminopropyl) carbodiimide (EDC), *N*-hydroxysuccinimide (NHS), fluorescein isothiocyanate isomer I (FITC), FITC-dextran (≈ 70×10^3 g mol^{-1}), dimethylsulfoxide (DMSO), nitric acid (HNO_3), NaOH (1 N), and acetic acid were purchased from Sigma Aldrich (St. Quentin Fallavier, France). Methanol (HPLC grade) and acetonitrile were purchased from Carlo Erba® (Val de Reuil, France). Isobutyl cyanoacrylate monomer was purchased from Afinitica Technologies (Barcelona, Spain). Polyfluor 570 (methacryloxyether thiocarbamyl rhodamine B) was purchased from Biovalley Polyscience Inc (Warrington, USA). A-float-layer dialysis device (≈ 3×10^5 g mol^{-1}) was purchased from Spectrum Labs (Rancho Dominguez, CA, USA). Dialysis membranes with molecular weight cutoffs ≈ 1×10^5 g mol^{-1}, ≈ 12×10^3 g mol^{-1}, and ≈ 3×10^3 g mol^{-1} were purchased from Spectra/Por (Biovalley, Marne la Vallée, France). A dialysis membrane with a molecular weight cutoff ≈ 1×10^3 g mol^{-1} was purchased from Spectrum-Labs (New Jersey, USA). Syringe filters (30 mm, pore size 1 µm PTFE membrane, non-sterile) were purchased from Sigma Aldrich (St. Quentin Fallavier, France). Milli-Q® water was used for all the experiments (Resistivity 18.2 MΩ.cm at 21 °C, Millipore purification system, Millex, SLAP 0225, Millipore, France).

2.2. Reagents for cell culture

Murine hematopoiesis-derived macrophages (J774A.1) were from CLS (Eppelheim, Germany). Dulbecco-modified eagle medium (DMEM), streptomycin, and penicillin were purchased from ThermoFisher Scientific (Illkirch, France). Phosphate buffer saline (PBS, pH 7.4), fetal bovine serum (FBS), trypan blue, and 3-[4,5- dimethylthiazol-2-yl]-2,5-diphenyl tetrazolium bromide (MTT) were from Sigma Aldrich (St. Quentin Fallavier, France). Penicillin/streptomycin solution contains 10,000 units of penicillin and streptomycin dissolved in a citrate buffer at a concentration of 10 mg mL^{-1}.

3. METHODS

3.1. Polysaccharide chemical coupling of FITC

3.1.1. Chitosan labeling

The reaction between the isothiocyanate group of FITC Isomer I and the primary amine groups of the D-glucosamine units of chitosan was performed according to the method developed elsewhere.[18, 19] Powder of chitosan (200 mg) was dispersed in 20 mL of acetic acid (0.1 mol L^{-1}) in an amber flask and under magnetic stirring (400 rpm). Then, methanol (20 mL) was added, followed by a slow addition of 10 mL of a solution of FITC in methanol at a concentration of 2 mg mL^{-1}. The reaction was left to proceed for 3 h, protected from light. The reaction was stopped, and the labeled chitosan was precipitated by raising the pH to ~ 9 - 10 by adding drop-by-drop NaOH solution (1 N). FITC grafted chitosan was centrifuged at 4500 × *g* for 30 min at 25 °C and washed 3 times with acetic acid to eliminate unreacted components. The products were re-dispersed in 20 mL of acetic acid (0.1 mol L^{-1}) and dialyzed against water for 3 days (molecular weight cutoff ≈ 3×10^3 g mol^{-1}). The obtained FITC-chitosan was freeze-dried for 24 h (Alpha 1-2 freeze-dryer, Fisher Scientific Bioblock, Illkirch, France).

3.1.2. Hyaluronan labeling

Hyaluronan (400 mg) was dissolved in water (60 mL) in an amber flask. Then, a solution of NHS (8.63 mg) and EDC (14.37 mg) in water (2.5 mL) was added to the hyaluronan solution and magnetically stirred for 30 min at 25 °C to activate the carboxylic groups on hyaluronan. Then, a solution containing FITC (50 mg) was dissolved in DMSO (70 mL) (equivalent to 2.5% moles of the disaccharides units) was added dropwise to the previously prepared mixture. The reaction occurs at 25 °C under magnetic stirring (300 rpm) for 12 h. At the end of the reaction, the FITC-labeled hyaluronan was dialyzed against water for 32 h (Dialysis membrane with a molecular weight cutoff ≈ 1×10^3 g mol^{-1}). This dialysis step will eliminate DMSO, and other impurities produced by NHS

and EDC. In this dialysis step, water was changed after 1 h, 3 h, 5 h, and overnight. To eliminate any residual FITC that did not react with hyaluronan, PD-10 desalting columns (Sephadex G-25, GE Healthcare Life Sciences, Amersham, UK) were used to separate the eluted product from the unreacted molecules, which stack in the stationary phase. Water was used as the mobile phase. The obtained products were freeze-dried for 24 h.

3.2. Preparation of NS and E-NM

3.2.1. NS preparation

NS composed of PIBCA core and polysaccharide shell were prepared using an anionic emulsion polymerization of isobutyl cyanoacrylate monomer and the polysaccharides in an acidic medium. This method was adapted from previous reports using other polysaccharides, including chitosan [14, 15], dextran [16], and hyaluronan [17]. Non-labeled NS and FITC-labeled NS were prepared by dissolving 69 mg of each polysaccharide (FITC-labeled or not) in 5 mL of dilute nitric acid at a concentration of 0.2 M under magnetic stirring (300 rpm) in a glass tube at 40 °C for 30 min. After polysaccharide dissolution, 250 μL of isobutyl cyanoacrylate monomer was added under vigorous magnetic stirring (adjusted to 750 rpm). After firmly closing the vials, the reaction continued at 40 °C under stirring for 24 h. The sample was cooled to room temperature. Then, nanospheres were purified first by filtration through a 1 μm filter to remove polymer aggregates and then by dialysis using a Spectra/Por membrane with a molecular weight cutoff $\approx 100 \times 10^3$ g mol^{-1} twice for 30 min, twice for 60 min, and once overnight against 1 L of water. The pH of the final suspension was adjusted to 6.3 - 6.5 with NaOH (0.02 N). The concentration of the NS in the suspensions was 18 mg mL^{-1}, as evaluated by freeze-drying.

NS labeled with rhodamine (denoted as Rh-labeled) were prepared similarly, except that 5 min after adding isobutyl cyanoacrylate, a solution of PolyFluor 570 (1 mL) (a fluorescent competitive monomer at a 2 mg mL^{-1} concentration in acetonitrile) was added. The reaction continued at 40 °C

under magnetic stirring for 24 h. Then, the NS were purified by filtration followed by dialysis according to the process described above for non-labeled and FITC-labeled NS.

3.2.2. E-NM preparation

3.2.2.1. Optimization of the preparation of a stretchable film containing the NS

Ellipsoidal particles were obtained by the physical deformation of NS according to protocols published elsewhere.[11, 12] PVA film formulation was first optimized without adding NS. Homogeneity and sufficient stretchability of the films were the two target properties for optimizing the formulation and process parameters, as shown in Table S1. Optimized formulation parameters were the concentration and hydrolysis degree of PVA and the percentage of glycerol (Table S1). Briefly, solutions of PVA were prepared by dissolving PVA powders in water at different temperatures (20 °C, 40 °C, 50 °C, and 75 °C). Mixing duration was also optimized (from 4 to 12 h). The plasticizer was then added to the PVA solution under magnetic stirring. The formulation was observed visually for each parameter, and only homogenous solutions were selected for film casting and stretching experiments.

3.2.2.2. Preparation of PVA film containing the NS

First, a PVA solution was prepared by adapting protocols reported in the publications of Champion et al.,[20] and Ahmed et al.[12] Briefly, 20 mL of water was added to 2 g of PVA powder (87 - 90% hydrolyzed) under magnetic stirring for 1 h at room temperature (20 °C). Then, 440 mg of glycerol was added to the mixture. Glycerol was used as a plasticizer to decrease the T_g of the PVA film.[20] The final mixture was magnetically stirred at room temperature for 16 h to obtain a homogenous solution. The concentrations of PVA and glycerol were 10 wt% and 2 wt%, respectively. Then, a suspension of NS (720 µL) was dispersed in 1 mL of this solution to reach a final concentration of 13 wt% of NS per PVA solution.[11, 12] The resulting mixture of NS and PVA/glycerol solution was gently stirred for 30 min, spread on a glass slide (25 × 75 mm), and dried for 12 h at 37 °C to evaporate water. After drying, the films were immediately recovered from the glass slide and placed in a

thermoregulated stretching machine. Film stretching was operated at 50 °C, and the stretching speed was 0.5 mm min^{-1}. Ellipsoidal NM were obtained by stretching the films in one axis (*x, x'*) to a final length of 130 mm. At the end of the stretching, the films were immediately detached from the machine and rapidly cooled to 5 °C using a flux of cold air using dry ice (temperature -16.5 °C) while the films were maintained at the maximum stretched position. After cooling, the film was recovered in 1 mL of water. The recovered film was poured into a folate A-lyser dialysis device (molecular weight cutoff $\approx 300 \times 10^3$ g mol^{-1}) after its initial preparation according to the manufacturer's instructions. The dialysis was maintained for 24 h. The pH of the obtained suspensions was then adjusted to 6.5 with NaOH 0.1 N. To investigate the effect of PVA on NS surface modification, cytotoxicity, and endocytosis, NS were immersed in PVA and purified using the above-described protocol.

3.3. Physicochemical characterizations

3.3.1. Quasi-elastic light s&cattering

NS mean hydrodynamic diameters were measured in a Zetasizer Nanoseries (Nano-ZS, Malvern Instruments, France). Samples (100 µL) were diluted in 1 mL of water before measurement at 25 °C. The scattered angle was 173°.

3.3.2. Surface potential

Zeta (ζ) potential measurements characterize the surface potentials of NS and E-NM were characterized by electrophoretic mobility. This method was already used for surface potential characterization of spherical and nonspherical NM [21-24]. The ζ potentials were calculated at 25 °C by measuring the electrophoretic mobility using an electrophoretic light scattering technique (Zetasizer Nanoseries Nano-ZS, Malvern Instruments, France). For sample preparation, 60 µL of each suspension was diluted with 2 mL NaCl (1 mM). Then, 1 mL of each suspension was placed in a disposable folded capillary cell. The scattered angle was 173°. Each experiment was replicated three times on three independent formulations.

3.3.3. Transmission electron microscopy

TEM was used in this investigation to characterize NS and E-NM's shape, size, and aspect ratio of nonspherical NM. TEM characterizations were performed at 80 kV transmission using a transmission electron microscope (JEOL 1400) coupled to TEM Domain Centre software. The suspensions were diluted in water (1/10 for NS and E-NM). The dilution was optimized to observe particles with good contrast. Then, 25 µL NS and E-NM suspensions were placed on a carbon grid and stained with phosphotungstic acid 1% (pH 7.4) before observation. The grid was then placed on a slide and inserted into the microscope for observation. Different frames were randomly selected for each TEM microphotograph set to analyze the geometrical dimensions of NS or E-NM ($n > 100$ particles). Size distribution analysis was performed on TEM images using ImageJ and fitted to a normal Gaussian law. Statistical analyses were performed using GraphPad Prism software.

3.3.4. ITC

An isothermal calorimeter (VP-ITC, MicroCal Inc., USA) has been used for characterizing the interaction of polysaccharides with PVA. A typical experiment used a syringe filled with 250 µL of chitosan, dextran, or hyaluronan (0.5 mM) aqueous solution to titrate an aqueous solution of PVA (1 mM) into the calorimetric cell at 293.15 K (20 °C) or 323.15 °K (50 °C). Aliquots of 10 µL of titrant (polysaccharide solution) were delivered over 20 s, intervals between injections were 180 s, and agitation speed was 310 rpm. A background titration was obtained by injecting polysaccharide solution in water in the sample cell.

3.4. Cell culture

3.4.1. Cell growth conditions

Cells were incubated at 37 °C in a humidified atmosphere (5% CO_2). Cells were maintained in cell culture flasks (75 cm^2, Sigma Aldrich, St. Quentin Fallavier, France) and passaged every three days, reaching 70 - 80% confluency. Cells were cultured on DMEM supplemented with 10% FBS, 100 µg mL^{-1} streptomycin, and 100 IU mL^{-1} penicillin.

3.4.2. Cytotoxicity assay

In vitro cytotoxicity was investigated using the MTT assay. Macrophages were first cultured in 96-well at 10^3 cells/well concentration. The plates were preincubated for 48 h at 37 °C. Then, NS before and after their soaking in PVA and E-NM, as well as their negative controls (native polysaccharides), were diluted in the culture medium to reach the following concentrations (0.1, 0.5, 1, 10, 25, 50, 100, and 250 µg mL^{-1}). After 24 h of incubation of each preparation with the cells, 20 µL of an MTT solution in PBS (5 mg mL^{-1}) was added to each well. After two hours of incubation, the content of the wells was removed, and 200 µL DMSO was added to solubilize the forzman crystals that formed after adding the MTT reagent. Then, 96-well plates were stirred at 450 rpm for 30 min. After that, the absorbances of solubilized formazan crystals were measured with a microplate reader at 570 nm. IC_{50} values (concentration of each preparation to reduce cell viability by 50% relative to untreated control cells, respectively) were calculated from the dose-response curve. All experiments were repeated six times.

3.4.3. Particle endocytosis

Cells were analyzed in a CytoFlex cytometer (Beckman-Coulter) driven by Cytexpert 2.4 software for endocytosis studies. Cells were excited by a 488 nm laser for fluorescence measurements, and fluorescence emission was collected through a 525/40-nm bandpass filter. FITC-labeled preparations were incubated at 37 °C with cells to measure endocytosis efficiency. After a washing step, cells were resuspended in PBS, and 0.01% trypan blue was added to quench FITC fluorescence outside the cells. The threshold of positive cells was determined by comparison with cells without preparations. Frequency (F) and Mean Fluorescence Intensity (MFI) were used to calculate an internalization index (I) ($I = F \times MFI$). For each condition, a total of 15,000 - 20,000 cells were analyzed. The effect of the particle morphology on internalization in macrophages was studied on hyaluronan NS pre-incubated in PVA and purified hyaluronan E-NM. The polysaccharide composition (hyaluronan) was kept

constant while the concentrations varied as 0.1, 1, or 10 μg mL^{-1}. The incubation duration was kept constant at two hours.

3.5. Data analysis

Graphics of cellular viability and aspect ratio were analyzed by using Graphpad prism®. Graphics that compare the cellular viability of the two cell lines after treatment with the different types of particles and negative controls were performed with R programming language using "dplyr" package to manipulate data, ''ggplot2'' package to plot data, and ''gridExtra'' package to pool data in comparative graphics.

4. RESULTS AND DISCUSSION

In this investigation, two NM morphologies were designed: spherical and ellipsoidal. Surface properties were tailored using different polysaccharides, namely chitosan, dextran, and hyaluronan. Each type of particle was conjugated to FITC to monitor NM cell internalization by flow cytometry. The fluorescence-quenching method was employed to distinguish between NM attached to the cell surface and those ingested by the cell. This method involves adding a component that quenches the fluorescence of attached FITC-conjugated NM while the ingested particles remain fluorescent.[25] Trypan blue, a non-permeant dye, quenched membrane-bound fluorescein-labeled compounds for flow cytometry analyses. Trypan blue is known to quench the green fluorescence of cell-surface attached particles.[26] Dextran and hyaluronan were conjugated with FITC, while dextran-FITC was commercially available. The three FITC-labeled polysaccharides were then used for the preparation of FITC-labeled NM.

4.1. NS and E-NM preparation and physicochemical characterizations

4.1.1. NS

4.1.1.1. Mean hydrodynamic diameter

Spherical particles were designed by emulsion polymerization of isobutylcyanoacrylate. Representative TEM images of non-labeled NS and FITC-labeled NS are given in Figure 1. FITC labeling slightly affected the mean hydrodynamic diameter of NS (Table 1). The labeling used in this

299 investigation differed from the one reported earlier with PIBCA NS.[27] In most reports on
300 fluorescently labeled PIBCA NS, a fluorescent monomer is added to the polymerization medium,
301 which competes with PIBCA during polymerization. However, this strategy significantly increased the
302 mean hydrodynamic diameter of NS, as observed from the size measurement in Table 1. The mean
303 hydrodynamic diameter of rhodamine-labeled NS rose from 197 to 388 nm for chitosan and 126 to
304 326 nm for dextran. Hyaluronan NS showed an increase in mean hydrodynamic diameter from 355 to
305 984 nm (Table 1).

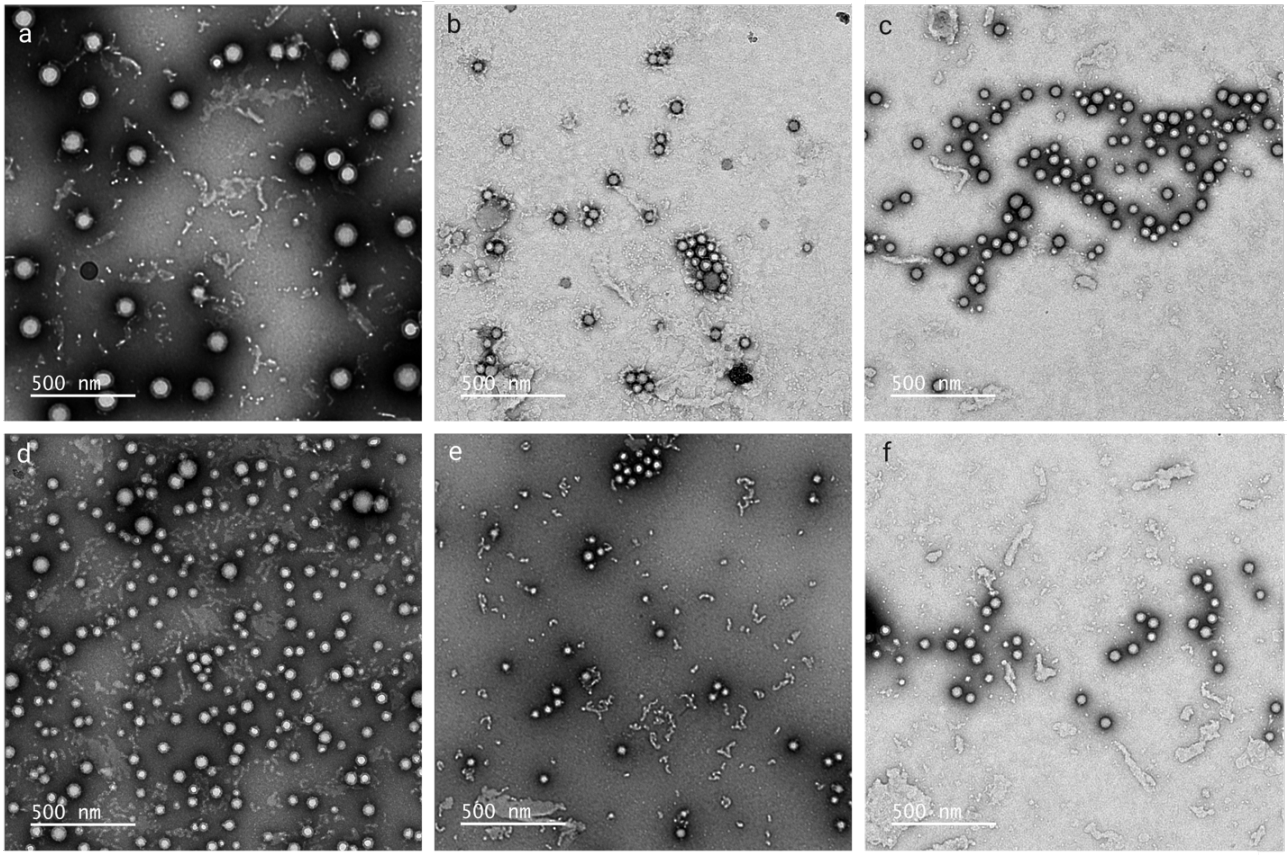

306 **Figure 1:** Representative TEM images of non-labeled NS (a,b,c), and FITC-labeled NS (d,e,f),
307 composed of PIBCA and chitosan (a,d), dextran (b,e), and hyaluronan (c,f).

4.1.1.2. ζ potential

Before labeling, chitosan NS exhibited a ζ potential of +35.5 mV due to the protonated amine groups at the pH of 6.3 - 6.5.[28] NS coated with dextran displayed a negative ζ potential (-5.6 mV), which agrees with previous findings.[29, 30] Hyaluronan NS exhibited a strong negative charge (-39.9 mV) (Table 1) due to carboxylic groups of hyaluronan.[31] Chemical structures of chitosan, dextran, and hyaluronan are given in Figure S2.a,b, and c, respectively. NS labeling with FITC decreased the ζ potential of chitosan NS from $+35.5$ mV to $+27.2$ mV. FITC grafting on the primary amine groups of chitosan could explain this decrease in the ζ potential. Similarly, FITC resulted in a reduction of the ζ potential of NS composed of dextran and hyaluronan. This decrease in the ζ potential could be due to the presence of carboxylic groups of the FITC isomer I grafted on the polysaccharides.

Table 1: Effect of labeling method on mean hydrodynamic diameter (d_h) and zeta potential (ζ) of NS prepared by polymerizing IBCA and chitosan, dextran, or hyaluronan. The polysaccharides were labeled or not with FITC (FITC-labeled) or rhodamine (Rh-labeled). *n = 3* different preparations.

Physicochemical parameter	Chitosan			Dextran			Hyaluronan		
	Non-labeled	FITC-labeled	Rh-labeled	Non-labeled	FITC-labeled	Rh-labeled	Non-labeled	FITC-labeled	Rh-labeled
d_h (nm)	197 ± 8	153 ± 2	388 ± 37	126 ± 25	116 ± 2	326 ± 21	355 ± 5	358 ± 11	984 ± 22
ζ (mV)	+35.5 ± 2.7	+27.9 ± 0.5	+40.5 ± 0.2	-5.6 ± 0.2	-12.4 ± 0.7	-2.1 ± 0.8	-39.9 ± 3.0	-42.6 ± 2.1	-41.0 ± 0.5

Table 2: Physicochemical properties of NS and E-NM prepared by polymerizing IBCA and chitosan, dextran, or hyaluronan. The polysaccharides were labeled or not with FITC. *n = 3* different preparations.

Particle morphology	Physicochemical parameter	Chitosan		Dextran		Hyaluronan	
		Non-labeled	FITC-labeled	Non-labeled	FITC-labeled	Non-labeled	FITC-labeled
NS	d_h^a (nm)	197 ± 8	153 ± 2	126 ± 25	116 ± 2	355 ± 5	358 ± 11
	d_{TEM} (nm)	85 ± 25	80 ± 17	59 ± 7	51 ± 6	62 ± 8 [a]	59 ± 13
E-NM	w_{TEM} (nm)	310 ± 97	127 ± 50	95 ± 31	96 ± 38	106 ± 42 [b]	67 ± 28
	h_{TEM} (nm)	64 ± 15	51 ± 18	40 ±10	50 ± 15	44 ± 13 [b]	28 ± 9
	Γ	4.9 ± 0.9	2.5 ± 0.4	2.4 ± 0.5	1.9 ± 0.4	2.4 ± 0.6	2.4 ± 0.7
	Γ_{min} - Γ_{max}	3.5 - 7.6	1.6 - 4.1	1.6 - 4.0	1.1 - 3.3	1.6 - 4.0	1.3 - 3.9
NS	ζ potential (mV)	+35.5 ± 2.7 [a]	+27.9 ± 0.5 [a]	-5.6 ± 0.3 [a]	-12.4 ± 0.7 [a]	-39.9 ± 3.0 [a]	-42.6 ± 2.1 [a]
		+5.8 ± 0.2 [b]	+1.7 ± 0.3 [b]	-1.2 ± 0.2 [b]	-1.4 ± 0.1 [b]	-28.3 ± 3.1 [b]	-17.9 ± 3.6 [b]
		+2.7 ± 0.6 [c]	+5.4 ± 0.1 [c]	-2.0 ± 0.9 [c]	-7.1 ± 0.6 [c]	-32.1 ± 0.8 [c]	-34.3 ± 1.4 [c]
E-NM		+1.5 ± 0.2 [d]	+1.4 ± 2.1 [d]	-1.9 ± 1.0 [d]	-5.6 ± 1.0 [d]	-32.4 ± 1.1 [d]	-36.4 ± 2.1 [d]

d_h: mean hydrodynamic diameter.

d_{TEM}: particle diameters determined by analyzing TEM images of NS. $n > 100$ particles analyzed.

Γ: aspect ratio calculated by dividing the mean width of E-NM (w_{TEM}) by the mean height of E-NM (h_{TEM}).

a: as prepared, without purification.

b: NS after incubation with PVA/glycerol solution (10/2 wt%). PVA hydrolysis degree was 87 - 90%.

c: NS after incubation with PVA/glycerol solution and purification by dialysis (cutoff $\approx 3 \times 10^5$ g mol^{-1}).

d: E-NM obtained after incubation of NS with PVA/glycerol solution (10/2 wt%) followed by drying and film stretching at 50 °C.

4.1.1.3. TEM

TEM analysis allowed the characterization of NS morphology and the diameter of individual particles. The NS size obtained from TEM images is denoted d_{TEM}. The results in Table 2 revealed that particle diameters obtained from TEM images were lower than the mean hydrodynamic diameters determined by QELS. Indeed, the QELS technique does not distinguish between an individual particle and an aggregate of several particles.

This difference is particularly marked for hyaluronan NS, where the d_h was equal to 355 nm for non-labeled particles while the d_{TEM} was 62 nm. Similarly, for FITC-labeled NS composed of hyaluronan, d_h was equal to 358 nm while d_{TEM} was 59 nm. This discrepancy could be attributed to the swelling behaviors of hyaluronan present on the NS surface during QELS measurements, leading to the formation of a gel-like layer around the NS during QELS measurements. It has been demonstrated that low hyaluronan molecular weight (~ 50 - 60 × 10^3 g mol^{-1}), similar to the molecular weight of hyaluronan used in this investigation, has a higher volumetric swelling ratio than high molecular weight (~ 10^6 g mol^{-1}).[32, 33] According to phantom network models, mesh sizes for hyaluronan 6×10^4 g mol^{-1}, 5×10^5 g mol^{-1}, and 10^6 g mol^{-1} were 35 ± 2, 24 ± 3, and 13 ± 1 nm, respectively.[33]

4.1.2. E-NM

4.1.2.1. Optimization of the formulation of homogenous and stretchable PVA film

In this section, we aimed to optimize PVA molecular weight and its degree of hydrolysis to obtain films with optimized characteristics suitable for producing ellipsoidal particles by stretching parent NS. An ideal film should dissolve at room temperature (*e.g.*, 20 °C), be homogeneous after drying, and resist stretching. The chemical structure of PVA is given in Figure S2.d, and the equation to calculate the degree of hydrolysis is in Eq.S1 (Supporting data). Different grades of PVA with variable degrees of hydrolysis were tested to optimize film formulation. The concentrations of PVA and glycerol, used as a plasticizer, were optimized.

Furthermore, the temperature and duration of mixing were modified to identify the best parameters for film formation. For each parameter, the homogeneity of the resulting solutions was observed visually. Then, the impact of each parameter on the film's stretchability was observed.

Varying the degree of hydrolysis from 80% to 100% revealed that the water solubility of PVA decreased when the hydrolysis degree increased (Table S1). Those results are explained by highly hydrolyzed PVA's high degree of crystallinity. Partially hydrolyzed PVA (80% and 87 - 90% of hydrolysis degrees) were soluble in water under magnetic stirring at 20 °C (Table S1 in the Supporting Information). Higher hydrolysis grades of PVA (99% or 100%) were insoluble in water at 20 °C, 40 °C, and 50 °C (Table S1). They are soluble at temperatures above 75 °C after 6 - 12 h of magnetic stirring. A higher crystallinity is due to the formation of strong inter and intra-chain hydrogen bonding. Thus, a high degree of hydrolysis requires higher temperatures for dissolution by disrupting inter and intra-hydrogen bonding.[34] The films obtained with partially hydrolyzed PVA (87 - 90%) were homogeneous, non-sticky, and smooth. In particular, the film obtained with partially hydrolyzed PVA at a concentration of 10 wt% was easily stretchable. In contrast, the films obtained with a lower PVA concentration (5 wt%) were thin and brittle when stretched. At a concentration of 5 wt%, fully hydrolyzed PVA and 99 wt% hydrolyzed PVA formed homogeneous and easily stretchable films. This difference could be explained by the higher molecular weight of fully hydrolyzed PVA and 99 wt% hydrolyzed PVA (89 - 98 $\times 10^3$ g mol^{-1}) compared with partially hydrolyzed PVA (87 - 90%), where the molecular weight was (30 - 70 $\times 10^3$ g mol^{-1}). This difference also explains why the 80% hydrolyzed PVA concentration required to form a stretchable film was 20 wt%. Probably because its molecular weight was (9 - 10 $\times 10^3$ g mol^{-1}), which is ten-fold lower than fully hydrolyzed and 99% hydrolyzed PVA.

Glycerol was added to the PVA solutions at different concentrations ranging from 0.5 to 2 wt%. Without glycerol, the films were brittle and fragile upon stretching. Notably, the films prepared with fully hydrolyzed and 99 wt% hydrolyzed PVA and supplemented with 2 wt% of glycerol were easily

stretchable. However, they dissolved at 75 °C after 12 h of magnetic stirring. They were not selected for the following experiments. The final PVA solution formulation used for the subsequent experiments was composed of PVA (87 - 90%) at 10 wt% in water and glycerol (2 wt%).

4.1.2.2. ζ potential characterization after NS incubation with PVA solution

In the article of Ahmed et al.,[12] we suggested that the PVA in the STBT® film adsorbed on the particle surface of chitosan NS. Herein, we measured the surface potentials of NS composed of chitosan, dextran, and hyaluronan before and after incubation with PVA solution. PVA solution was prepared according to the previous section. Once soaked into the PVA solution, we noticed a net decrease in the values of ζ potentials of chitosan NS from +35.5 mV to +5.8 mV for non-labeled chitosan NS and from +27.9 mV to +1.7 mV for FITC-labeled chitosan NS. The results are shown in Table 2 and Figure 2. Then, NS suspensions were purified by dialysis, and the efficacy of NS purification from PVA was estimated from the change in the NS ζ potential measurement before and after dialysis. The results in Table 2 and Figure 2 revealed that dialysis did not allow a complete purification of chitosan NS suspension from PVA since the ζ potentials were +2.7 mV and +5.4 mV for non-labeled and FITC-labeled chitosan NS, respectively.

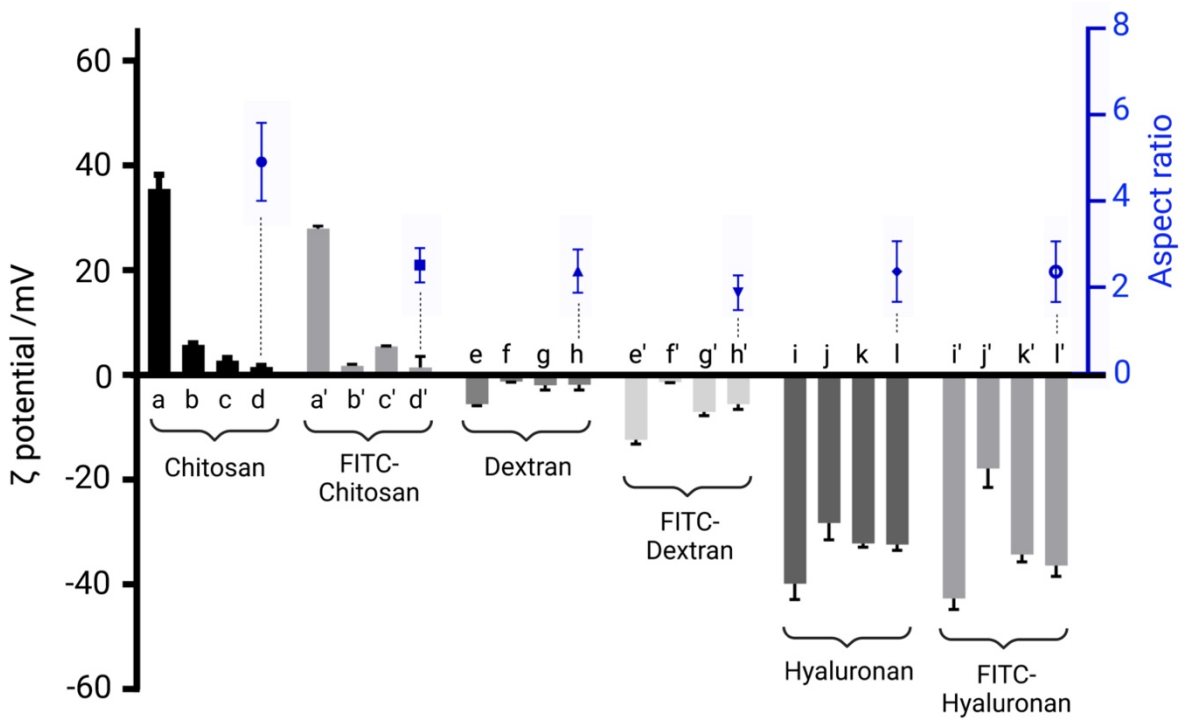

Figure 2: Representation of the effect of incubation of nanospheres with PVA on ζ potential (left y axis) and impact of polysaccharide type on the aspect ratio (right y axis). The preparations are composed of chitosan (a,b,c,d), FITC-chitosan (a',b',c',d'), dextran (e,f,g,h), FITC-dextran (e',f',g',h'), hyaluronan (i,j,k,l), and FITC-hyaluronan (i',j',k',l'). The preparations were composed as prepared nanospheres (NS) without PVA (chitosan NS in (a), FITC-chitosan NS in (a'), dextran NS in (e), FITC-dextran NS in (e'), hyaluronan NS in (i), FITC-hyaluronan NS in (i')), NS after incubation with PVA denoted as NS+PVA (chitosan NS+PVA in (b), FITC-chitosan NS+PVA in (b'), dextran NS+PVA in (f), FITC-dextran NS+PVA in (f'), hyaluronan NS+PVA in (j), FITC-hyaluronan NS+PVA in (j')). NS after incubation with PVA and purification by dialysis denoted as NS_{PVA} (chitosan NS_{PVA} in (c), FITC-chitosan NS_{PVA} in (c'), dextran NS_{PVA} in (g), FITC-dextran NS_{PVA} in (g'), hyaluronan NS_{PVA} in (k), FITC-hyaluronan NS_{PVA} in (k')). Ellipsoidal nanomaterials denoted as E-NM (chitosan E-NM in (d), FITC-chitosan E-NM in (d'), dextran E-NM in (h), FITC-dextran E-NM in (h'), hyaluronan E-NM in (l), FITC-hyaluronan E-NM in (l')). ζ potential was the mean of $n = 3$ different preparations. Aspect ratio (Γ) was the mean of $n > 100$ particles analyzed.

Concerning NS composed of dextran, after incubation with PVA, the ζ potential varied from -5.6 mV to -1.2 mV for non-labeled dextran NS and from -12.4 mV to -1.4 mV for FITC-labeled dextran NS. Interestingly, purification of NS suspension by dialysis decreased the ζ potential from -1.2 mV to -2.0 mV for non-labeled dextran NS and from -1.4 mV to -7.1 mV for FITC-labeled dextran NS. In the case of dextran, purification was most effective in recovering the initial surface potential compared to chitosan. Similar observations were reported with hyaluronan NS. Indeed, the ζ potential

varied from -39.9 mV to -28.3 mV after incubation with PVA. Purification of NS suspension decreased the ζ potential from -28.3 mV to -32.1 mV for non-labeled hyaluronan NS and from -17.9 mV to -34.3 mV for FITC-labeled hyaluronan NS. For dextran and hyaluronan, purification by dialysis brings the ζ potential to values close to the ones reported with NS before incubation. The difference in the ζ potential before incubation and after purification is less marked than with chitosan. Those results could be attributed to the stronger interaction of PVA with chitosan than with dextran and hyaluronan on the NS surface. Consequently, the purification of chitosan NS after PVA adsorption is less efficient than dextran and hyaluronan. To explore this hypothesis, the interaction of PVA with the three polysaccharides was studied by ITC, as detailed in the following section.

4.1.2.3. ITC

ITC titration curves and enthalpies of the interactions of PVA with chitosan, dextran, and hyaluronan solutions are shown in Figure 3. The interaction was studied at 20 °C to mimic the temperature of NS incubation with PVA and at 50 °C to mimic the stretching temperature. The results revealed that the interaction of PVA was higher with chitosan than with dextran and hyaluronan at both temperatures, 20 °C and 50 °C (Figure 3). Strong interaction of PVA with chitosan could be due to hydrogen-bound formation between hydroxyl groups of PVA with amine groups, hydroxymethyl groups, hydroxyl groups, or carboxylic acid groups on chitosan. Those findings agree with data from the literature demonstrating that -CH_2-OH groups on PVA interacted with hydroxymethyl groups[35] and amine groups on chitosan.[36] Figure 3 revealed that the interaction of chitosan with PVA was higher at 50 °C (Figure 3.d) than at 20 °C (Figure 3.a). This behavior could be due to the decreased viscosity of PVA[34] and chitosan solutions[37] upon temperature increase. The interaction of PVA with dextran and hyaluronan solutions was lower than with chitosan at 20 °C (Figure 3.b,c) and 50 °C (Figure 3.e,f). The heat flows fall in the same range as dextran and hyaluronan dilution curves in water (Figure S3).

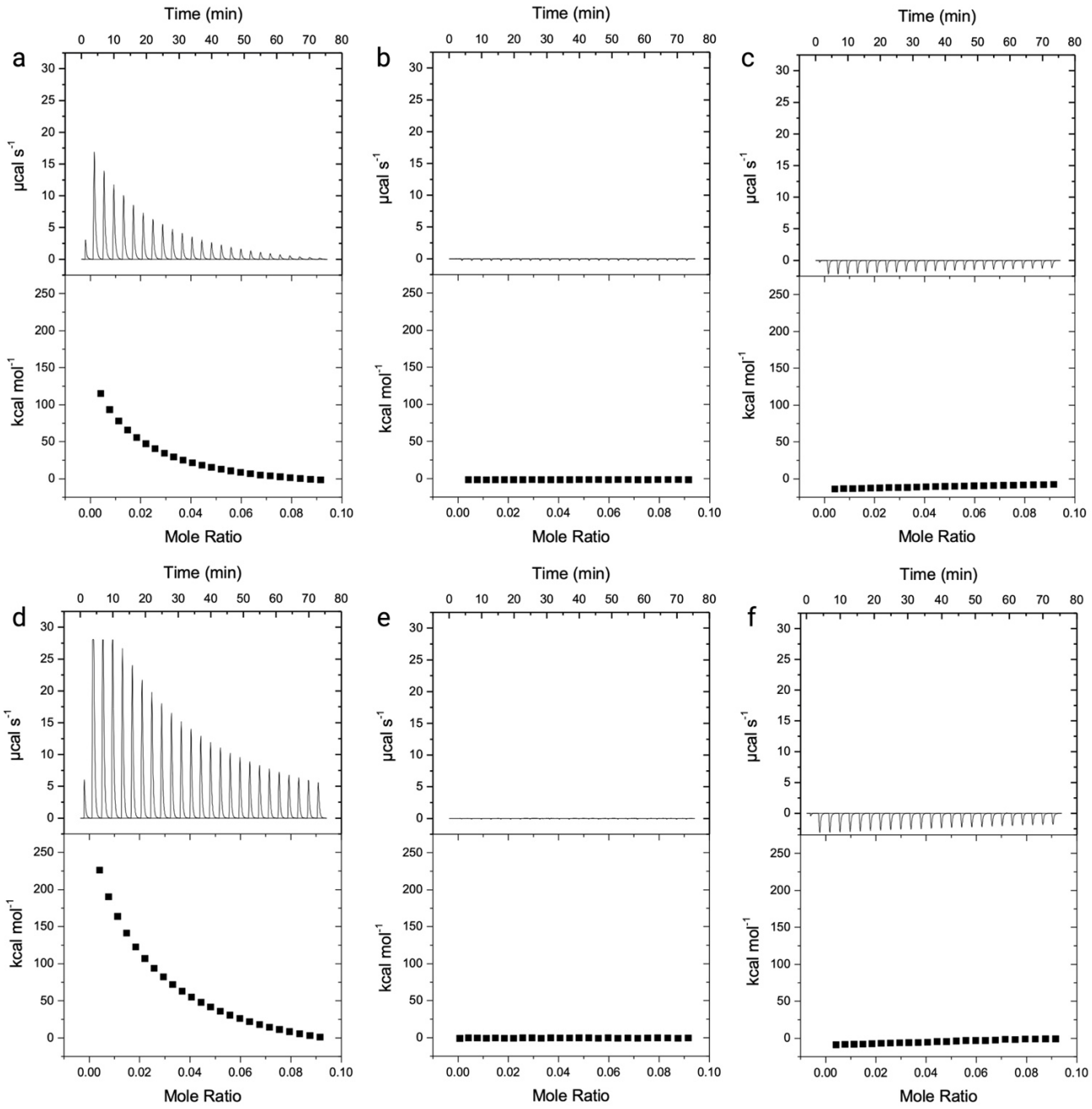

439

440 **Figure 3:** ITC titration curves and enthalpies of the interaction of PVA with chitosan (a,d), dextran
441 (b,e), and hyaluronan (c,f). The concentration of chitosan, dextran, and hyaluronan in the syringe was
442 0.5 mM, while the concentration of PVA in the titration cell was 1 mM. The temperature of the
443 experiment was maintained constant at 20 °C (a,b,c) or 50 °C (d,e,f).

444 **4.1.2.4. Physicochemical characterizations of E-NM**

445 In this section, E-NM were characterized by determining ζ potential, morphology, and dimensions
446 from TEM images. The ζ potentials of the E-NM reported in Table 2 and Figure 2 were in the same
447 range as spherical particles after incubation with a PVA solution and purification by dialysis.

Electrophoretic mobility was already used to characterize spherical and nonspherical NM surface potential.[21, 22]

The size of nonspherical particles was analyzed from TEM images. Indeed, the non-sphericity of NM complexifies their physicochemical characterizations compared with spherical particles. In many analytical techniques, the particles were assimilated to spheres. For example, in the quasi-elastic light scattering technique, the hydrodynamic size (d_h) is calculated from the diffusion coefficient (D_t) of the NM in suspension using the Stokes-Einstein equation $d_h = \frac{K_B T}{3\pi\eta D_t}$, where K_B is the Boltzmann constant, T the temperature and η the dynamic viscosity of the suspension. When dealing with the characterization of nonspherical particles, more relevant methods are required for analyzing shape, morphology, and size distribution. Transmission electron microscopy is a rapid and straightforward technique for characterizing the size of NM with a spherical or nonspherical morphology. TEM analysis of preparations composed of chitosan, dextran, hyaluronan, and FITC-labeled counterparts revealed that ellipsoidal particles were obtained by the physical deformation of parent NS regardless of the polysaccharide used (Figure 4). However, we observed that chitosan E-NM in Figure 4.a were well stretched compared with dextran and hyaluronan E-NM in Figure 4.b and 4.c, respectively. In the case of dextran and hyaluronan, the ellipsoids appeared less stretched than with chitosan. In Figure 4.b, dextran ellipsoids appeared more round-shaped than with chitosan. Calculation of the mean long axis dimension (width, w_{TEM}) and the mean small axis dimension (height, h_{TEM}) of more than 100 E-NM revealed that chitosan ellipsoids had the highest width (310 ± 97 nm) compared with the width of dextran (95 ± 31 nm) and hyaluronan (106 ± 42 nm). The aspect ratios (Γ) were calculated by dividing w_{TEM} by h_{TEM} for each preparation. The mean aspect ratios of more than 100 particles observed from TEM images are reported in Table 2.[12] The results indicated that the mean aspect ratio of non-labeled chitosan E-NM (4.9 ± 0.9) was higher than the ones obtained with dextran (2.4 ± 0.5) and hyaluronan (2.4 ± 0.6). This difference was visible by plotting the mean aspect ratios in Figure 2 (right *y* axis).

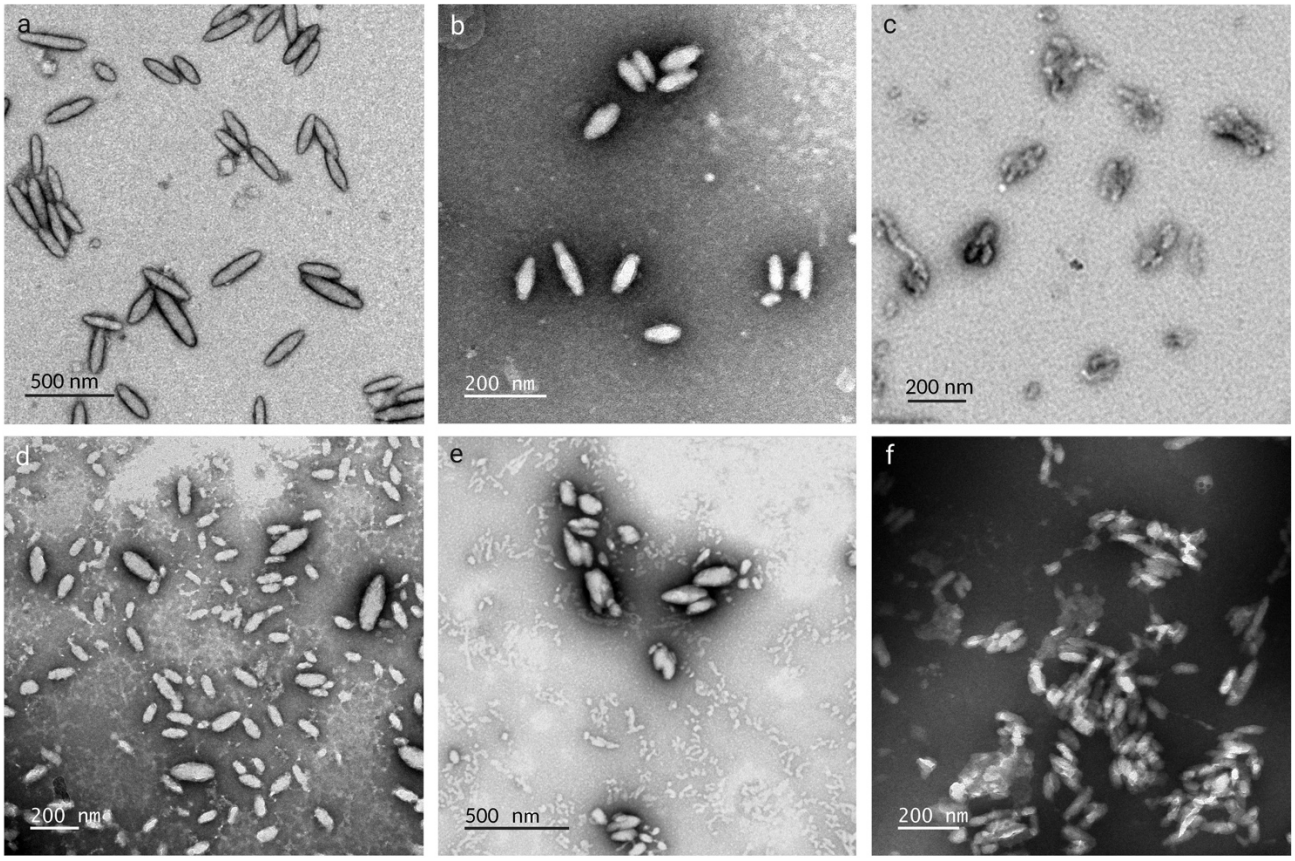

Figure 4: Representative TEM images of non-labeled E-NM (a,b,c) and FITC-labeled E-NM (d,e,f), composed of PIBCA and chitosan (a,d), dextran (b,e), and hyaluronan (c,f).

The results also revealed that the FITC grafting of chitosan decreased the mean aspect ratio from (4.9 ± 0.9) to (2.5 ± 0.4). We suspected that the decrease in the mean aspect ratio is correlated to the change in the ζ potential. Consequently, we plotted the mean aspect ratio on the same figure as the ζ potential. In Figure 2 and Table 2, we noticed a decrease in the mean aspect ratio of chitosan ellipsoids due to FITC grafting. Indeed, FITC Isomer I was grafted on the NH_2 groups of chitosan, which could reduce the interacting sites with PVA. Lower interaction with PVA results in a lower aspect ratio. Those findings suggest that high ζ potential could result from high interaction with PVA. The reduced aspect ratio in the case of dextran and hyaluronan could be due to a lower interaction of those polysaccharides with PVA, as characterized by ITC in the previous section. In the case of chitosan, FITC grafting on amine groups reduces the ζ potential and, in turn, the interaction with PVA.

We also noticed that the change in the aspect ratio was slightly influenced by the T_g. Indeed, the T_g of PIBCA was 46 °C.[38] The T_g of chitosan was in the range of 140 ~ 150 °C,[39] while the T_g of dextran was 149 °C.[40] Concerning hyaluronan, the T_g was observed at -70 °C to -100 °C.[41]

4.2. Cytotoxicity

Herein, the cytotoxicity of NS and E-NM was investigated in macrophages. Cytotoxicity was also investigated for native polysaccharides used as controls. As expected, native polysaccharides were non-toxic toward macrophages in the tested concentration range (Figure 5) since the IC_{50} values were higher than 250 μg mL^{-1} (Table 3). As the PVA modifies the particle's surface potential, the effect of the particle incubation in PVA solution on the cell viability was investigated. Figure 5 represents the relative cell viability curves of NS and E-NM composed of PIBCA. Analysis of IC_{50} values revealed that regardless of the polysaccharide type, the as-prepared PIBCA NS, without incubation with PVA solution, caused significant cell death in a concentration-dependent fashion (Figure 5). We noticed the presence of a threshold concentration around 1 μg mL^{-1}, beyond which the percentage of cell viability starts to decrease drastically for both cell lines (Figure 5). The cytotoxicity mechanism of cyanoacrylate polymers was attributed to their degradation, suggesting that the degradation products are responsible for the toxicity.[42] In particular, the cytotoxicity of poly(isobutyl 2-cyanoacrylate) polymers was attributed to formaldehyde release upon polymer degradation.[42] Other investigations suggested that the cytotoxicity observed with cyanoacrylate polymers may be due to cellular damage leading to oxidative conversion of membranal lipids.[43]

Interestingly, this investigation revealed that NS cytotoxicity was reduced after incubating with PVA solution, followed by purification. The IC_{50} values were reported in Table 3 and Figure 6. Analysis of the results in Table 3 and Figure 6 revealed that regardless of the polysaccharide type, the particles denoted as NS_{PVA}, had a higher IC_{50} than prepared NS (Table 3). Reduced cytotoxicity could be due to the adsorption of the PVA on the NS surface, as discussed in the previous section. Those findings also suggested that PVA was not entirely removed from the preparation after purification by

dialysis. The dose-response cytotoxicity curves in Figure 5 revealed that the ellipsoidal shape of the E-NM did not significantly modify their cytotoxicity in both cell lines compared with NS_{PVA}. The values of the IC_{50} were in the same range for NS_{PVA} and E-NM (Table 3 and Figure 6). This result could be due to comparable surface properties of NS incubated with PVA and E-NM due to the PVA adsorption, which partially masked the polysaccharide on the particle surface. Considering those results, we can conclude that cytotoxicity is linked to the particle's surface properties rather than morphology.

Table 3: IC_{50} values (μg mL^{-1}) after 24-h-incubation of macrophages J774A.1 with polysaccharide preparations composed of chitosan, dextran, and hyaluronan. For each polysaccharide, the preparations were composed of solutions, nanospheres as prepared (NS), and nanospheres after incubation with PVA and purification (denoted as NS_{PVA}). The IC_{50} values were obtained from relative cell viability curves in Figure 5.

Preparations		**IC_{50} (μg mL^{-1})***
Chitosan preparations	Solution	> 250
	NS [a]	5.0
	NS_{PVA} [b]	34.2
	E-NM	39.5
Dextran	Solution	> 250
	NS [a]	12.3
	NS_{PVA} [b]	38.4
	E-NM	43.2
Hyaluronan	Solution	> 250
	NS [a]	7.5
	NS_{PVA} [b]	107.2
	E-NM	109.4

*: Macrophages RAW264.7

[a]: as prepared

[b]: NS were previously incubated with PVA/glycerol (10/2 wt%) solution and dialyzed. PVA hydrolysis degree was 87 - 90%.

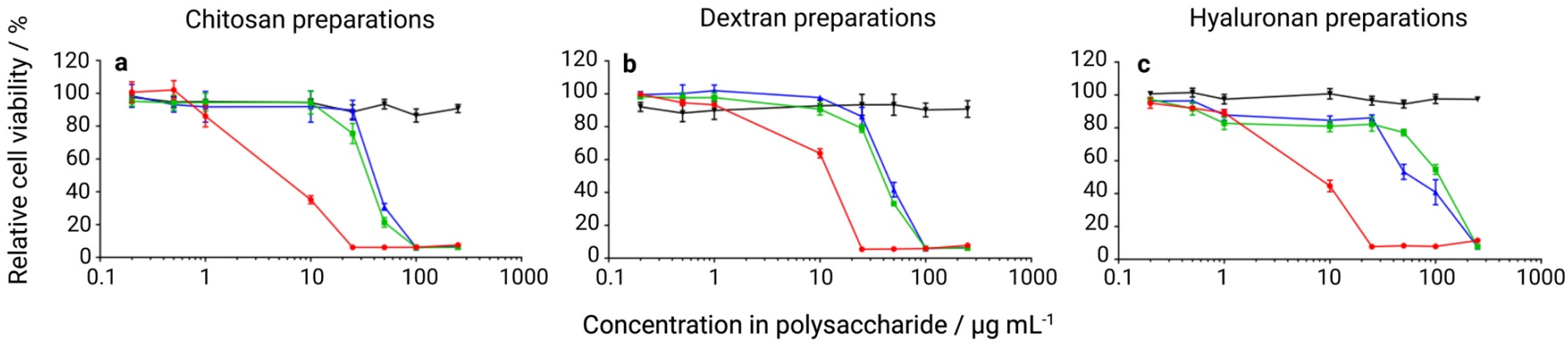

526

527 **Figure 5:** Macrophage viability testing of polysaccharide preparations composed of chitosan (a), dextran (b), and hyaluronan (c). The preparations
528 were composed of native polysaccharides (black q, corresponding to chitosan solution in (a), dextran solution in (b) and hyaluronan solution in
529 (c)), NS without PVA (red l, corresponding to chitosan NS in (a), dextran NS in (b) and hyaluronan NS in (c)), NS after incubation with PVA,
530 denoted as NS_{PVA} (green n, corresponding to chitosan NS_{PVA} in (a), dextran NS_{PVA} in (b) and hyaluronan NS_{PVA} in (c)), and elongated nanomaterials
531 (blue p, corresponding to chitosan E-NM in (a), dextran E-NM in (b) and hyaluronan E-NM in (c)). The incubation duration was kept constant at
532 24 h. Data are presented as the mean ± s.d. (n = 6 independent experiments).

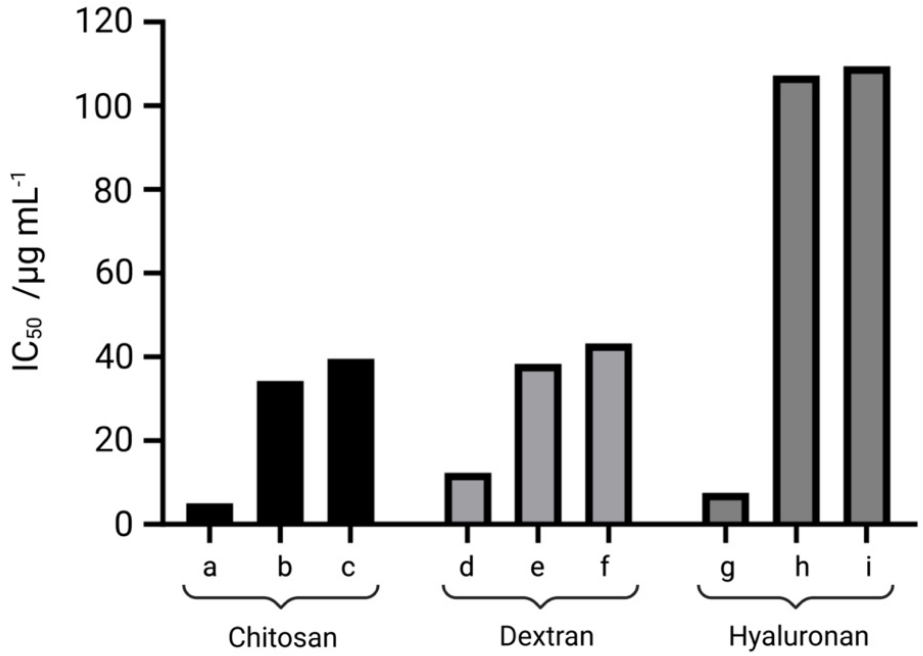

Figure 6: IC_{50} values (µg mL^{-1}) after incubation of macrophages J774A.1 with polysaccharide preparations composed of chitosan (a,b,c), dextran (d,e,f), and hyaluronan (g,h,i). The preparations were composed of nanospheres as prepared (NS) without PVA (chitosan NS in (a), dextran NS in (d) and hyaluronan NS in (g)), NS after incubation with PVA, denoted as NS_{PVA} (chitosan NS_{PVA} in (b), dextran NS_{PVA} in (e) and hyaluronan NS_{PVA} in (h)). The incubation duration was kept constant at 24 h. Data are presented as the mean of $n = 6$ independent experiments). The IC_{50} values were obtained from relative cell viability curves in Figure 5.

4.3. Cell internalization

The polysaccharide composition was kept constant, and NM morphology was modified for the following experiments. Hyaluronan was selected because its interaction with cells involves several types of receptors called hyaladherins. Hyaladherins include CD44,[44] CD38, RHAMM (receptor for hyaluronan-mediated motility, designated as CD168), stabilin-2,[45] lymphatic vessel endothelial hyaluronan receptor (LYVE-1), inter-α-inhibitor (IαI), and TSG-6 (tumor necrosis factor-stimulated gene-6). Internalization of hyaluronan NS_{PVA} and E-NM by macrophages was studied at three particle concentrations (0.1, 1, and 10 µg mL^{-1}). The results in Figure 7, presenting the internalization index before and after trypan blue quenching, revealed that NS_{PVA} and E-NM were internalized by macrophages for the tested concentrations. At concentrations of 0.1 µg mL^{-1} and 1 µg mL^{-1}, before trypan blue quenching, internalization indexes of E-NM were in the same order of magnitude as NS_{PVA}. However, after adding trypan blue, internalization indexes of E-NM were reduced for both

concentrations, while internalization indexes of NS_{PVA} increased (Figure 7). At a high concentration of 10 µg mL^{-1}, E-NM adsorption to macrophages was higher than $NS_{PVA,}$ while the internalization index drastically reduced for E-NM after trypan blue quenching. Those results could be due to the difference in the actin structures formed upon particle interaction with the macrophage surface. Indeed, among the four endocytosis mechanisms of NM (micropinocytosis, clathrin-mediated, caveolae-mediated, translocation), micropinocytosis is the most reported mechanism for NM, with a size ranging from 200 nm to 5 µm.[4, 46] Macropinocytosis is mostly initiated by actin-driven membrane ruffles (Figure 8.a).

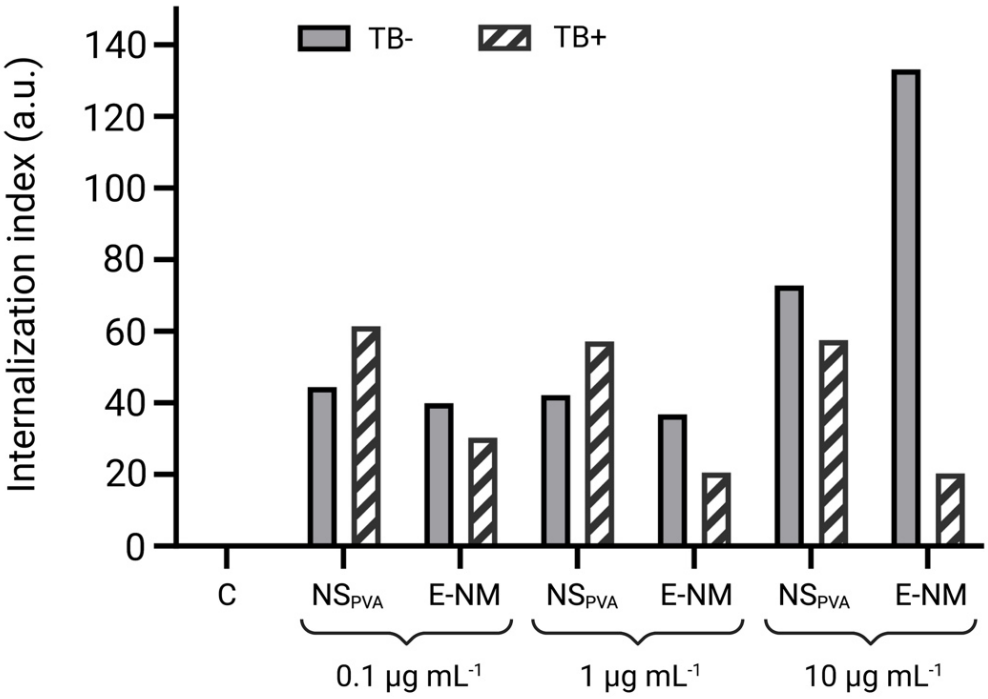

Figure 7: Effect of particle concentration and morphology on internalization index in macrophages without adding trypan blue (TB-) and after adding trypan blue (TB+). Macrophages were incubated 2 h with preparations composed of FITC-hyaluronan nanospheres after incubation with PVA and purification by dialysis (NS_{PVA}) and ellipsoidal nanomaterials (E-NM). The concentration of each preparation was varied as 0.1, 1, and 10 µ mL^{-1}. The internalization index was calculated by multiplying the percent of fluorescent cells with fluorescence intensity and normalized by taking the internalization index of cells without particles at 100%. Control experiment (C) comprised macrophage suspension without adding hyaluronan preparations. At least 50 cells were counted for each sample.

We hypothesize that E-NM could spread on the macrophage surface by particle long axis (Figure 8). Consequently, actin polymerized at points of contact failed to create the adequate actin structure necessary to engulf the particle (Figure 8). Another hypothesis to explain those findings is the surface

property of the E-NM. According to previous investigations,[47] the hypothesis of the organization of hyaluronan at the surface of the NS is given in the article of Coty and coworkers.[48] Film stretching technique could result from a stretching of hyaluronan located at the surface of the E-NM. Consequently, the interaction of hyaluronan with hyaladherins located on the macrophage surface could be lowered. Regardless of the phagocytosis mechanism of hyaluronan E-NM was reduced, limiting capture by macrophages could be advantageous since phagocytosis can create a substantial barrier to successful drug delivery. In some applications, macrophage internalization of particles is necessary.[49, 50] However, phagocytosis could prevent particles from releasing the encapsulated active drug near or within the desired cell population if macrophages are not the targeted cell type. Consequently, those findings could be exploited to reduce phagocytosis compared with conventional NS.

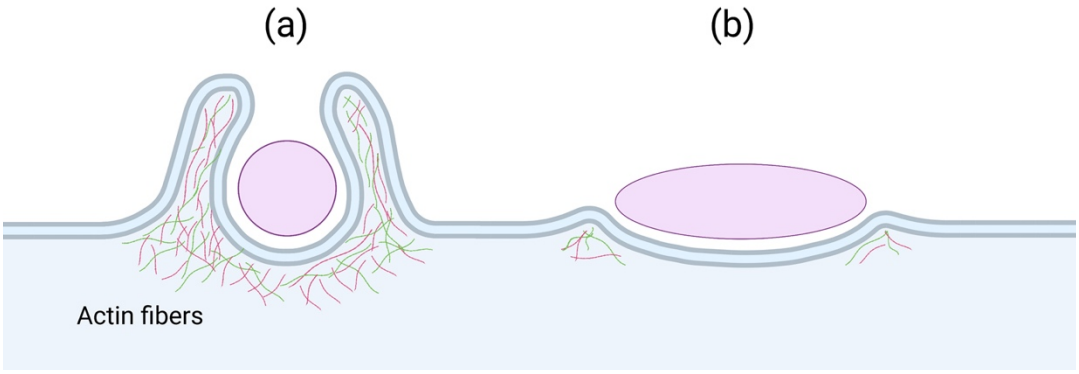

Figure 8: Schematic representation of hypothesis of the interaction of a nanosphere (a) and an ellipsoidal nanomaterial (b) with macrophage surface and involvement of actin fibers.

5. CONCLUSION

The investigation unveiled a correlation between NS surface potential, aspect ratio, and the interaction of PVA and the polysaccharides. Spherical and ellipsoidal NM were designed with surface properties adjusted using different polysaccharides (chitosan, dextran, and hyaluronan). The NM were labeled with FITC to track their internalization by cells. The FITC grafting on the NS surface resulted in modifications to the surface potential, while the size was relatively unchanged. Transmission electron microscopy analysis provided insights into the size and morphology, particularly for

ellipsoidal particles, revealing aspect ratio variations influenced by polysaccharide type and FITC grafting. Indeed, high PVA interaction with chitosan led to a high aspect ratio (4.9), while lower interaction resulted in a lower aspect ratio (2.4). Future investigations could predict the aspect ratio of ellipsoidal NM by studying the interaction of NS surfaces with the dispersing polymer.

Cytotoxicity studies demonstrated reduced toxicity after incubating NS with a PVA solution and subsequent purification, indicating the potential of PVA adsorption on NM surfaces to mitigate their toxic effects. Cell internalization experiments revealed that NS, after PVA incubation, were internalized by macrophages. However, ellipsoidal NM exhibited lower internalization than NS, despite having comparable surface potentials. This reduced phagocytosis of ellipsoidal NM may be attributed to their nonspherical morphology. This finding suggests a potential advantage for applications where macrophage internalization is undesirable. Future perspectives include visualizing the kinetics of NM interactions with cells, particularly NM with varying morphologies and surface properties. Developing stretchable polymers capable of interacting with NS surfaces would be interesting, allowing for their physical deformation during stretching. These polymers should be easily removable through conventional purification techniques to limit surface modification of stretched NM.

6. Funding

This work was supported by the Institut Universitaire de France, the ANR-17-CE09-0038 and ANR-21-CE09-0015.

7. Acknowledgements

The present work has benefited from the Imagerie-Gif core facility supported by l'Agence Nationale de la Recherche (ANR-11-EQPX-0029/Morphoscope, ANR-10-INBS-04/FranceBioImaging; ANR-11-IDEX-0003-02/Saclay Plant Sciences). The present work has benefited from the platform PIM of I2BC supported by French Infrastructure for Integrated Structural Biology (FRISBI) ANR-10-INBS-05. The authors thank Dr. Josh Mc Graw and Pr. Gilles Ponchel for scientific discussion and helpful advice.

8. Credit Author Statement

The manuscript was written through the contributions of all authors. All authors have given approval for the final version of the manuscript. ZA: Chemical modifications, formulation, characterization, data curation, formal and statistical analysis, writing original experimental section. HH: Chemical modifications, formulation, characterization, cell culture experiments, data curation, formal and statistical analysis, writing original experimental section. HK: Involvement in the data analysis and discussion. MB: Monitoring and data analysis of flow cytometry. K.B: Conceptualization; Data curation; Formal analysis; Funding acquisition; Investigation; Methodology; Project administration; Resources; Supervision; Validation; Visualization; Writing - original draft; Writing - review & editing.

9. REFERENCES

1. Huang, X., et al., *The landscape of mRNA nanomedicine.* Nature Medicine, 2022. **28**(11): p. 2273-2287.
2. Thapa, R.K. and J.O. Kim, *Nanomedicine-based commercial formulations: Current developments and future prospects.* Journal of Pharmaceutical Investigation, 2023. **53**(1): p. 19-33.
3. Veiga, N., Y. Diesendruck, and D. Peer, *Targeted nanomedicine: Lessons learned and future directions.* Journal of Controlled Release, 2023. **355**: p. 446-457.
4. Hadji, H. and K. Bouchemal, *Effect of micro- and nanoparticle shape on biological processes.* Journal of Controlled Release, 2022. **342**: p. 93-110.
5. Zhu, X., et al., *Non-spherical micro-and nanoparticles in nanomedicine.* Materials Horizons, 2019. **6**: p. 1094-1121.
6. Gagner, J.E., et al., *Effect of gold nanoparticle morphology on adsorbed protein structure and function.* Biomaterials, 2011. **32**(29): p. 7241-7252.
7. Chakraborty, S., et al., *Contrasting effect of gold nanoparticles and nanorods with different surface modifications on the structure and activity of bovine serum albumin.* Langmuir, 2011. **27**(12): p. 7722-7731.
8. Dutta, D., et al., *Adsorbed proteins influence the biological activity and molecular targeting of nanomaterials.* Toxicological Sciences, 2007. **100**(1): p. 303-315.
9. Ho, C., et al., *Preparation of monodisperse ellipsoidal polystyrene particles.* Colloid and Polymer Science, 1993. **271**(5): p. 469-479.
10. Champion, J.A. and S. Mitragotri, *Role of target geometry in phagocytosis.* Proceedings of the National Academy of Sciences, 2006. **103**(13): p. 4930-4934.
11. Palazzo, C., et al., *Obtaining nonspherical poly (alkylcyanoacrylate) nanoparticles by the stretching method applied with a marketed water-soluble film.* International Journal of Polymeric Materials and Polymeric Biomaterials, 2017. **66**(8): p. 416-424.
12. Ahmed, Z., G. Ponchel, and K. Bouchemal, *Shape stability of ellipsoidal nanomaterials prepared by physical deformation.* International Journal of Pharmaceutics, 2021. **609**: p. 121178.
13. Meyer, R.A., R.S. Meyer, and J.J. Green, *An automated multidimensional thin film stretching device for the generation of anisotropic polymeric micro-and nanoparticles.* Journal of Biomedical Materials Research Part A, 2015. **103**(8): p. 2747-2757.

14. Malli, S., et al., *Topically applied chitosan-coated poly(isobutylcyanoacrylate) nanoparticles are active against cutaneous Leishmaniasis by accelerating lesion healing and reducing the parasitic load.* ACS Applied Bio Materials, 2019. **2**(6): p. 2573-2586.
15. Malli, S., et al., *Surface-dependent endocytosis of poly(isobutylcyanoacrylate) nanoparticles by Trichomonas vaginalis.* International Journal of Pharmaceutics, 2018. **548**(1): p. 276-287.
16. Coty, J.-B., et al., *Characterization of nanomedicines' surface coverage using molecular probes and capillary electrophoresis.* European Journal of Pharmaceutics and Biopharmaceutics, 2018. **130**: p. 48-58.
17. Diaz-Salmeron, R., G. Ponchel, and K. Bouchemal, *Hierarchically built hyaluronan nano-platelets have symmetrical hexagonal shape, flattened surfaces and controlled size.* European Journal of Pharmaceutical Sciences, 2019. **133**: p. 251-263.
18. Qaqish, R. and M. Amiji, *Synthesis of a fluorescent chitosan derivative and its application for the study of chitosan–mucin interactions.* Carbohydrate Polymers, 1999. **38**(2): p. 99-107.
19. Ahmed, Z., et al., *New insights on the structure of hexagonally faceted platelets from hydrophobically modified chitosan and α-cyclodextrin.* International Journal of Pharmaceutics, 2018. **548**(1): p. 23-33.
20. Champion, J.A., Y.K. Katare, and S. Mitragotri, *Making polymeric micro-and nanoparticles of complex shapes.* Proceedings of the National Academy of Sciences, 2007. **104**(29): p. 11901-11904.
21. Barua, S., et al., *Particle shape enhances specificity of antibody-displaying nanoparticles.* Proceedings of the National Academy of Sciences, 2013. **110**(9): p. 3270-3275.
22. Gratton, S.E., et al., *The effect of particle design on cellular internalization pathways.* Proceedings of the National Academy of Sciences, 2008. **105**(33): p. 11613-11618.
23. Yoo, J.W., N. Doshi, and S. Mitragotri, *Endocytosis and intracellular distribution of PLGA particles in endothelial cells: effect of particle geometry.* Macromolecular Rapid Communications, 2010. **31**(2): p. 142-148.
24. Gratton, S.E., et al., *Microfabricated particles for engineered drug therapies: elucidation into the mechanisms of cellular internalization of PRINT particles.* Pharmaceutical Research, 2008. **25**(12): p. 2845-2852.
25. Hed, J., *The extinction of fluorescence by crystal violet and its use to differentiate between attached and ingested microorganisms in phagocytosis.* FEMS Microbiology Letters, 1977. **1**(6): p. 357-361.
26. Busetto, S., et al., *A single-step, sensitive flow cytofluorometric assay for the simultaneous assessment of membrane-bound and ingested Candida albicans in phagocytosing neutrophils.* Cytometry Part A: the journal of the International Society for Analytical Cytology, 2004. **58**(2): p. 201-206.
27. Bravo-Osuna, I., et al., *Mucoadhesion mechanism of chitosan and thiolated chitosan-poly(isobutyl cyanoacrylate) core-shell nanoparticles.* Biomaterials, 2007. **28**(13): p. 2233-2243.
28. de Alvarenga, E.S., *Characterization and properties of chitosan.* Biotechnology of biopolymers, 2011. **91**: p. 48-53.
29. Chauvierre, C., et al., *Novel polysaccharide-decorated poly (isobutyl cyanoacrylate) nanoparticles.* Pharmaceutical research, 2003. **20**(11): p. 1786-1793.
30. Sharma, A., et al., *Physical characterization and in vivo organ distribution of coated iron oxide nanoparticles.* Scientific reports, 2018. **8**(1): p. 1-12.
31. Diaz-Salmeron, R., et al., *Real-time visualization of morphology-dependent self-motion of hyaluronic acid nanomaterials in water.* International Journal of Pharmaceutics, 2021. **609**: p. 121172.
32. Burdick, J.A., et al., *Controlled degradation and mechanical behavior of photopolymerized hyaluronic acid networks.* Biomacromolecules, 2005. **6**(1): p. 386-391.
33. Browne, S., S. Hossainy, and K. Healy, *Hyaluronic Acid macromer molecular weight dictates the biophysical properties and in vitro cellular response to semisynthetic hydrogels.* ACS Biomaterials Science & Engineering, 2019. **6**(2): p. 1135-1143.
34. Briscoe, B., P. Luckham, and S. Zhu, *The effects of hydrogen bonding upon the viscosity of aqueous poly (vinyl alcohol) solutions.* Polymer, 2000. **41**(10): p. 3851-3860.

35. Jawalkar, S.S., et al., *Molecular modeling simulations to predict compatibility of poly (vinyl alcohol) and chitosan blends: a comparison with experiments.* The Journal of Physical Chemistry B, 2007. **111**(10): p. 2431-2439.
36. Srinivasa, P., et al., *Properties and sorption studies of chitosan–polyvinyl alcohol blend films.* Carbohydrate polymers, 2003. **53**(4): p. 431-438.
37. Desbrieres, J., *Viscosity of semiflexible chitosan solutions: Influence of concentration, temperature, and role of intermolecular interactions.* Biomacromolecules, 2002. **3**(2): p. 342-349.
38. Peracchia, M., et al., *Development of sterically stabilized poly (isobutyl 2-cyanoacrylate) nanoparticles by chemical coupling of poly (ethylene glycol).* Journal of Biomedical Materials Research: An Official Journal of The Society for Biomaterials and The Japanese Society for Biomaterials, 1997. **34**(3): p. 317-326.
39. Dong, Y., et al., *Studies on glass transition temperature of chitosan with four techniques.* Journal of Applied Polymer Science, 2004. **93**(4): p. 1553-1558.
40. Li, W., et al., *Effect of water sorption on glass transition and microstructural variation of dextran & sugar mixtures.* Carbohydrate Polymers, 2022. **290**: p. 119505.
41. Hatakeyama, T. and H. Hatakeyama, *PHASE TRANSITION OF SODIUM HYALURONATE, HYLAN AND POLYURETHANES DERIVED FROM HYALURONIC ACID IN THE PRESENCE OF WATER*, in *Hyaluronan*. 2002, Elsevier. p. 323-328.
42. Tseng, Y.C., et al., *In vitro toxicity test of 2-cyanoacrylate polymers by cell culture method.* Journal of biomedical materials research, 1990. **24**(10): p. 1355-1367.
43. Papatheofanis, F.J., *Cytotoxicity of alkyl-2-cyanoacrylate adhesives.* Journal of biomedical materials research, 1989. **23**(6): p. 661-668.
44. Bano, F., et al., *A single molecule assay to probe monovalent and multivalent bonds between hyaluronan and its key leukocyte receptor CD44 under force.* Scientific reports, 2016. **6**(1): p. 1-14.
45. Lee, G.Y., et al., *Hyaluronic acid nanoparticles for active targeting atherosclerosis.* Biomaterials, 2015. **53**: p. 341-348.
46. Haigler, H.T., J.A. McKANNA, and S. Cohen, *Rapid stimulation of pinocytosis in human carcinoma cells A-431 by epidermal growth factor.* The Journal of cell biology, 1979. **83**(1): p. 82-90.
47. Coty, J.-B., E.E. Oliveira, and C. Vauthier, *Tuning complement activation and pathway through controlled molecular architecture of dextran chains in nanoparticle corona.* International Journal of Pharmaceutics, 2017. **532**(2): p. 769-778.
48. Coty, J.-B., M. Noiray, and C. Vauthier, *Assessment of complement activation by nanoparticles: development of a SPR based method and comparison with current high throughput methods.* Pharmaceutical research, 2018. **35**(7): p. 129.
49. Mukherjee, N., et al., *Host P2X7R-p38MAPK axis mediated intra-macrophage leishmanicidal activity of Spergulin-A.* Experimental Parasitology, 2022. **241**: p. 108365.
50. Yang, Z., et al., *Targeted delivery of antimicrobial peptide by Cry protein crystal to treat intramacrophage infection.* Biomaterials, 2019. **217**: p. 119286.

Supporting data

1. Optimization of the PVA film formulation

Table S1: Optimization of PVA film formulation. Formulation parameters were modified by adjusting the degree of hydrolysis, molecular weight, and concentration of PVA, and glycerol concentration. Process parameters were modified by adjusting the dissolution temperature and duration of stirring. Stirring speed was maintained at 400 rpm. Film stretchability was ranked as follows: brittle if the film cannot be manipulated and stretchable if the film can be deformed at least 2 folds without breaking up to this pre-set deformation.

PVA hydrolysis degree	Molecular weight $\times 10^3$ g mol^{-1}	[PVA] (wt%)	Glycerol (wt%)	Solubility of the preparation	T and stirring duration	Macroscopic aspect after drying	Handling	Detachment	Stretchability
80%	9 – 10	5	0	Soluble	20 °C, 3 h	Sticky, homogenous	+	Easy detachment	Brittle
			2	Soluble	20 °C, 3 h	Sticky, homogenous		Too sticky	Brittle
		10	0	Soluble	20 °C, 3 h	Sticky, homogenous		Easy detachment	Brittle
			2	Soluble	20 °C, 3 h	Sticky, homogenous		Too sticky	Brittle
		15	0.5	Soluble	20 °C, 3 h	Non sticky, homogenous		Easy detachment,	Rigid
			1	Soluble	20 °C, 3 h	Non sticky, homogenous		Easy detachment	Rigid
			2	Soluble	20 °C, 3 h	Non sticky, homogenous		Easy detachment	Slightly rigid
		20	0	Soluble	20 °C, 3 h	Non sticky, homogenous		Easy detachment	Tough
			0.5	Soluble	20 °C, 3 h	Non sticky, homogenous		Easy detachment	Good to stretching
			1	**Soluble**	**20 °C, 3 h**	**Non sticky, homogenous**		**Easy detachment**	**Good stretching**
			2	Soluble	20 °C, 3 h	Non sticky, homogenous		Easy detachment	Stretchable but rigid
87 – 90%	30 – 70	5	2	Soluble	20 °C, 6 h	Homogenous		Easy detachment	Good stretching but too much thin and flexible
		10	2	Soluble	20 °C, 6 h	Homogenous		Easy detachment	Good stretching
99%	89 – 98	5	2	Insoluble	40 °C, 6 h	Heterogenous, rough	-	Difficult detachment	Breaks during stretching
		5	2	Insoluble	50 °C, 6 h				
		5	2	Soluble	75 °C, 6 h	Homogenous smooth	+	Easy detachment	Good stretching
		10	2	Soluble	75 °C, 6 h				
100%		5	0	Insoluble	40 °C, 12 h	Heterogenous, rough	+	Difficult detachment	Breaks during stretching
		5	2	Insoluble	40 °C, 12 h		-		
		10	0	Insoluble	40 °C, 12 h		+		
		10	2	Insoluble	40 °C, 12 h		-		
		5	2	Soluble	75 °C, 12 h	Homogenous, smooth	+	Easy detachment	Good stretching
		10	2	Soluble	75 °C, 12 h				
(+): Recovered in one piece; (-): Cracks on film									

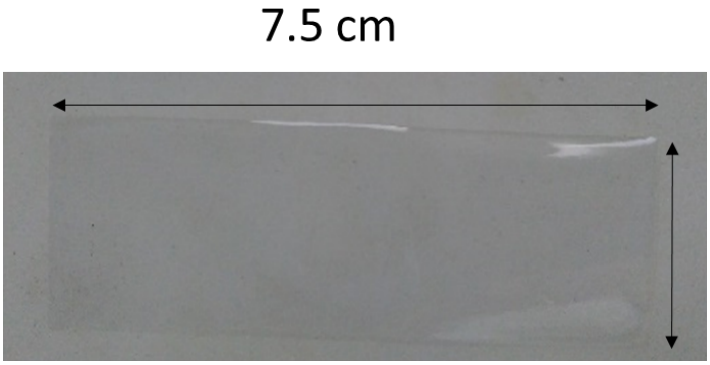

Figure S1: Photo of 87 – 90% hydrolysed PVA film before stretching. Film forming solution: 10 wt% PVA powder and 2 wt% glycerol.

2. Chemical structures of chitosan, dextran, hyaluronan and polyvinyl alcohol

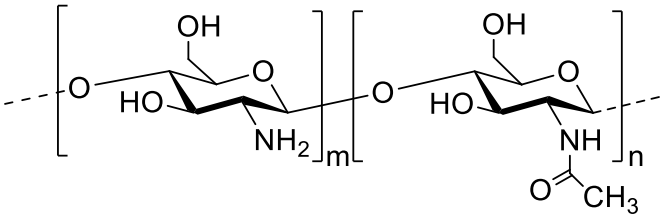

(a) Chitosan

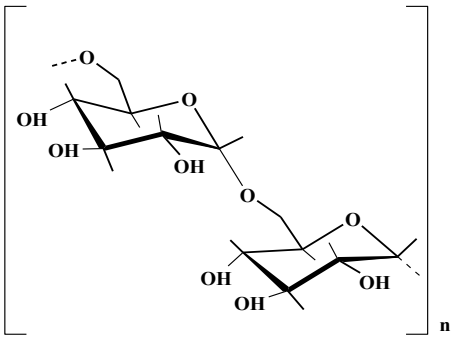

(b) Dextran

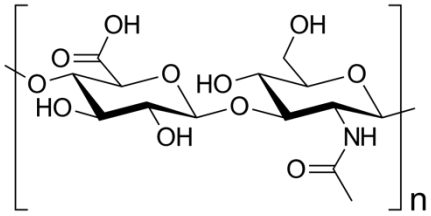

(c) Hyaluronan

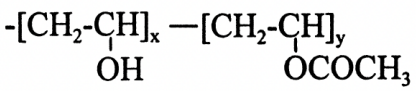

(d) Polyvinyl alcohol

Figure S2: Chemical structures of chitosan (a), dextran (b), hyaluronan (c), and polyvinyl alcohol (d). In (d), the degree of hydrolysis was calculated according to the equation Eq.S1 where x and y are the molar fractions of the hydroxyl and the acetate groups.

$$\text{PVA degree of hydrolysis} = \frac{x}{x+y} \qquad \text{Eq.S1}$$

3. ITC

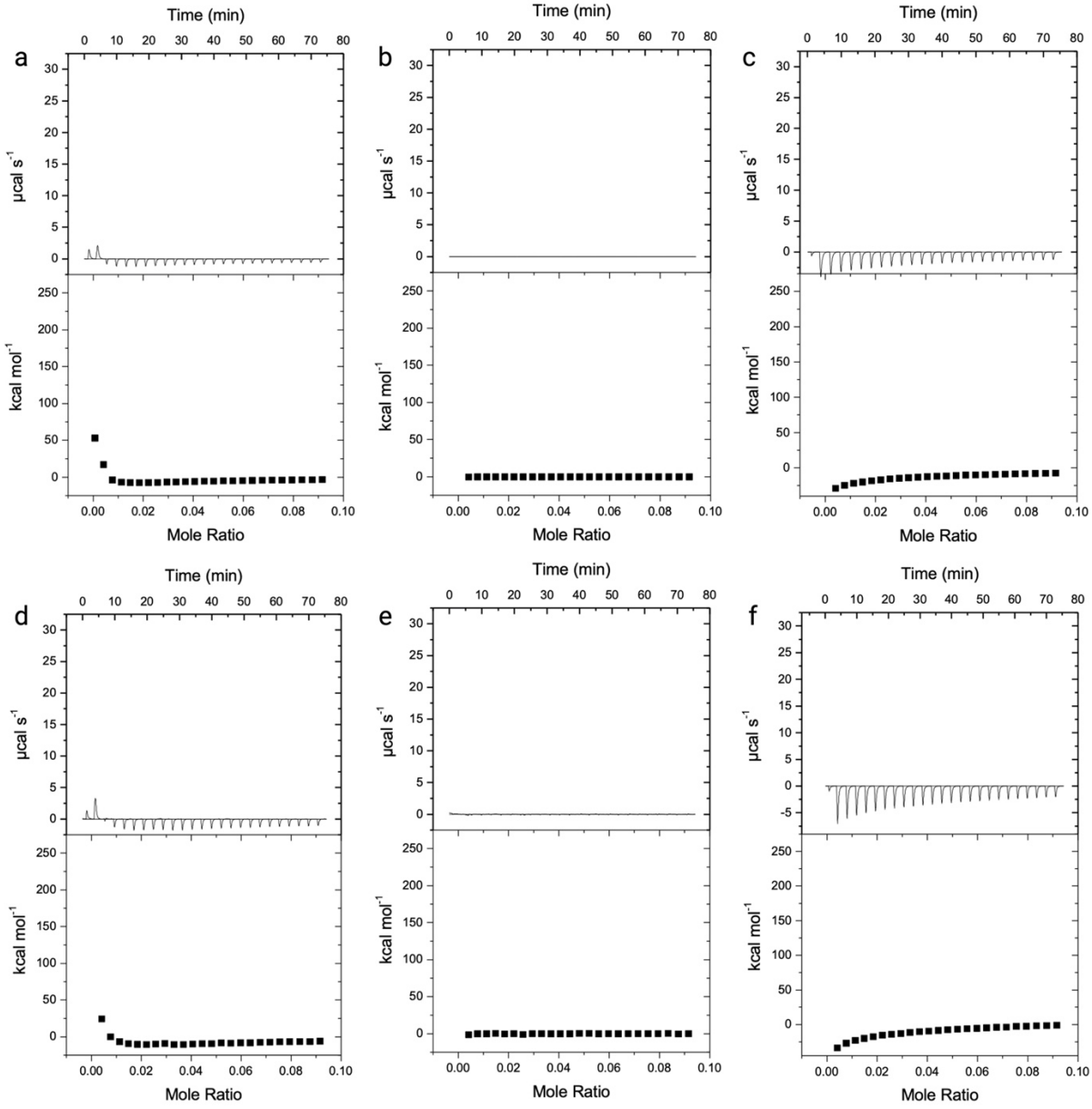

Figure S3: ITC titration curves and enthalpies of dilution of CS (a,d), DEX (b,e), and HA (c,f) in water. The concentration of CS, DEX, and HA in the syringe was 0.5 mM. Water was placed in the titration cell. The temperature of the experiment was maintained constant at 20 °C (a,b,c) or 50 °C (d,e,f).